Environmental Engineering and Management Journal
December 2018, Vol. 17, No. 12, 2837-2845
http://www.eemj.icpm.tuiasi.ro/; http://www.eemj.eu

"Gheorghe Asachi" Technical University of Iasi, Romania

INFLUENCE OF STIRRING SPEED AND GAS-TO-LIQUID RATIO ON ACTIVATED SLUDGE PERFORMANCE IN CARBAMAZEPINE ELIMINATION USING RESPONSE SURFACE METHODOLOGY AND PRINCIPAL COMPONENT ANALYSIS

Samer Semrany[1,2,3‡], Samir Taha[1], Hayet Djelal[2,3,4], Lidia Favier[2,3], Abdeltif Amrane[2*]

[1]Centre Azm pour la Recherche en Biotechnologie et ses Applications, LBA3B,
EDST Université Libanaise, Al-Mitein Street, Tripoli, Lebanon
[2]École Nationale Supérieure de Chimie de Rennes, Université de Rennes 1, Chimie et Ingénierie des Procédés,
CNRS UMR 6226, 11 Allée de Beaulieu, CS 50837, 35708 Rennes Cedex 7, France
[3]Université Européenne de Bretagne, 5 Boulevard Laënnec, 35000 Rennes, France
[4]Ecole des Métiers de l'Environnement, Campus de Ker Lann, 35170 Bruz, France

Abstract

Activated sludge (AS) is the mainly used biological process in water treatment; therefore, assessing the influence of various operating conditions on this process is relevant. This study aimed to evaluate at laboratory-scale the influence of the gas-to-liquid volume ratio ($R_{G/L}$) and the stirring speed (*SS*) on the biodegradation of carbamazepine (CBZ) by activated sludge. For this purpose, a central composite design (CCD) was used in association with response surface methodology (RSM). Batch cultures were carried out at room temperature for 21 days in a mineral medium of initial pH 7, containing CBZ at an initial concentration of 5 mg L^{-1} and a given amount of AS (achieving 0.05 AU at 600 nm). The two parameters *SS* and $R_{G/L}$ have been varied in the ranges of 80 to 320 rpm and 0.2 to 5, respectively. The pH, the (600 nm)-absorbance and the concentration of CBZ in the medium were monitored and their kinetics were modeled and linked to the operating conditions using principal component analysis (PCA). The obtained results showed that a low content of oxygen has a high positive effect, while an extreme stirring speed has a tiny negative effect on the process yield.

Key words: activated sludge, carbamazepine, composite central design, principal component analysis

Received: January, 2014; Revised final: October, 2014; Accepted: January, 2015; Published in final edited form: December 2018

1. Introduction

Activated sludge (AS) process is widely used in conventional biological treatment of wastewater. The organic compounds are degraded in activated sludge, aerobically or anaerobically. In fact, a consortium of microorganisms, mainly bacteria, is the basis of all current biological purification treatments. Biodegradation may be either complete (the pollutant is mineralized giving water, carbon dioxide and inorganic ions) or incomplete (the pollutant is degraded or partially transformed into organic metabolites), depending on the treated effluent (type and concentration of pollutants) and on the type of involved microorganisms (Chen et al., 2016; Crini and

---

[*] Author to whom all correspondence should be addressed: e-mail: abdeltif.amrane@univ-rennes1.fr; Phone: + 33 (0)2 23 23 81 55; Fax: + 33 (0)2 23 23 81 99

[‡] This paper is derived from the PhD thesis of the corresponding author, which is published online at: http://www.theses.fr/2014REN1S184.pdf

Badot, 2008; Ozkan-Yucel and Gokcay, 2017; Yu et al., 2016).

The presence of carbamazepine (CBZ), the main antiepileptic drug was repeatedly reported in various waters (Jones et al., 2002; Ferrari et al., 2004; Ternes, 1998; Yehya et al., 2015). This pharmaceutical is a slightly hydrophobic compound ($\log K_{o/w} = 2.45$), with negligible sorption capacities to the suspended solid particles of the activated sludge (Clara et al., 2004; Scheytt et al., 2005). Moreover, it is characterized by a weak solubility in water 17.7 mg L^{-1} to 112 mg L^{-1} (Ternes et al., 2002).

Concerning the elimination of carbamazepine (CBZ), advanced oxidation processes (AOPs), the photodegradation by solar or UV irradiation (in absence/presence of TiO_2), the ozonolysis (O_3), and the oxidation by ClO_2 have been tested by Ternes et al. (2002). In some cases, the results showed a high yield of elimination of CBZ; unfortunately, some of these oxidation by-products are more recalcitrant or toxic than their parent compound. For example, acridine and acridone, the by-products of the ozonolysis of CBZ are irritating, mutagenic and carcinogenic compounds (Rizzo, 2011). For that reason, AOPs are not appropriate for the elimination of this compound (Rehman et al., 2013). Therefore, the search for new and efficient solutions for their treatment remains a topic of interest.

On the other hand, various studies have shown the CBZ resistance to conventional treatments used in wastewater treatment plants (WWTPs) (Clara et al., 2004; Gebhardt and Schröder, 2007; Ternes, 1998). Indeed, this molecule was found in the effluents of these plants (up to 6.3 μg L^{-1}) (Ternes, 1998; Öllers et al., 2001), in surface water (up to 1.1 μg L^{-1}) (Ternes, 1998; Andreozzi et al., 2003; Metcalfe et al., 2003) and even in drinking water (30 ng L^{-1}) (Ternes, 2001).

According to the reviewed literature, the elimination of carbamazepine (CBZ) through an activated sludge process at WWTP scale did not exceed 16% (Gebhardt and Schröder, 2007; Kosjek et al., 2009). However, it would be interesting to assess the influence of the different operating conditions on this process in order to understand the source of this limited degradation. In fact, several operating parameters can affect the elimination yield of a given pollutant at both the large WWTP's scale and the laboratory's scale where the study usually starts in batch mode. The following four parameters appear to be the most influential: temperature, pollutant concentration, aeration rate, contact duration and spatial proximity between the purifying biomass in the AS and the pollutant.

The temperature, if moderately elevated, can accelerate the physical transfer phenomena and the rate of chemical and biochemical reactions. So the temperature appears to be the parameter of choice to optimize in laboratory study. Unfortunately, it is easy to control the temperature of a batch culture, but difficult at large scale such as in a WWTP, given the seasonal variations and the high cost of a system able to regulate and control this parameter for large volumes. Thus, optimizing the temperature at laboratory-scale is almost irrelevant since not really transposable to a WWTP.

Regarding the CBZ concentration, very low amounts (≈ 5 μg L^{-1}) are found in WWTP influents; infinity of other organic compounds that can be used by microorganisms for their metabolic needs are found in the treated water. Therefore, a recalcitrant pollutant such as CBZ will not be preferentially assimilated. For that reason, and to clearly highlight CBZ biodegradation trends, batch experiments carried out in this study were performed on a mineral medium, which did not contain organic matter other than the pollutant, to promote the consumption of carbamazepine. In addition, CBZ was added at a level one thousand fold above the concentrations usually observed in WWTPs in order to have enough material for a potential biomass growth in the absence of other readily biodegradable carbon source.

The contact between the purifying biomass and the pollutant is highly dependent on the biomass concentration, the residence time of the treated water in the basin, but also on the agitation speed. In a batch culture, this contact depends primarily on the stirring speed of the magnetic bar easily controlled at laboratory-scale. The aeration rate depends on the agitation but also on the intake of air blown by bubblers at the activated sludge basins. In the laboratory, and to simplify the design of batch cultures, no aeration system was used. However, the rate of aeration in a reactor which is close to the atmosphere can be easily correlated to the volume of the gaseous phase (the headspace of the culture).

Therefore, two parameters were chosen in order to explore the operating conditions influencing the yield of CBZ degradation by AS, the stirring speed (*SS*) and the gas-to-liquid volume ratio ($R_{G/L}$). An approach of central composite design (CCD) was used to find the individual effect of each of these factors and the effect of their interaction. Three parameters (pH, absorbance at 600 nm and CBZ residual concentration) were monitored during 21 days, and their kinetics was modeled. In a second step, the modeling of a polynomial response surface of second degree was considered to find the couples of conditions ($SS;\ R_{G/L}$) leading to extreme (maximum and minimum) CBZ biodegradation. Principal component analysis (PCA) has been performed to visualize different correlations among the system parameters. Finally, the whole kinetics of the system was linked to the operating conditions via multiple-linear regression, and a simplified mechanistic model was proposed in order to explain the system behavior.

2. Materials and methods

2.1. Experimental Approach

The used mineral culture medium contained in one liter of ultra-pure water (Milli-Q, United States) the following minerals (Riedel-de-Haën, Germany): 1 g of NaH_2PO_4, 2 g of NH_4Cl and 4 g of KNO_3. The target compound, carbamazepine (CBZ) in powder form (99 % purity) was purchased from Acros Organics (Geel, Belgium). Stock solution of CBZ at 1 g L^{-1} was prepared in pure ethanol and kept cool (4°C) until use. An adequate volume of this solution was spiked in the mineral medium to reach an initial concentration of 5 mg L^{-1}. The mixture pH was adjusted to 7. The culture medium was then sterilized in an autoclave (Raypa, Spain) at 121°C during 15 minutes to eliminate ethanol through volatilization. No thermal degradation of CBZ was observed during the sterilization process.

The used activated sludge was collected from a local WWTP (Tripoli, Lebanon) and maintained under aeration in a reactor of 10 L. A volume of 100 mL of sludge was centrifuged (4000 rpm, 5 min) and the supernatant containing organic matter was removed. The sludge was subsequently washed three times with distilled water and then re-suspended in 20 mL of distilled water. The culture medium was inoculated with an adequate volume of this suspension in order to obtain an initial (600 nm)-absorbance of 0.05 absorbance unit (AU).

The inoculated culture medium was then distributed into 12 Erlenmeyer flasks of identical capacity 500 mL following various volumes repartition (V_L = 100, 220, 300, 380 and 500 mL). These volumes corresponded to different gas-to-liquid volume ratios ($R_{G/L}$ = 0.2, 0.579, 1, 1.73 and 5) respectively. Indeed, when a culture of liquid volume V_L is placed in a closed container of total volume V_T = 600 mL, the headspace representing the gaseous phase volume is $V_G = (V_T – V_L)$ (Fig. 1-a) and hence the gas-to-liquid volume ratio is $R_{G/L} = V_G/V_L$.

Regarding the stirring speed, various rates were considered (SS = 80, 100, 200, 300 and 320 rpm) (WiseStir SMHS, Germany), in order to deal with the points of the design of experiments represented in Fig. 1-b. Samples were periodically taken during 21 days (at instants t = 0, 3, 7, 10, 14, 17 and 21 days) to monitor changes in the pH (pH-meter Orion 5 Star, Thermo Scientific, Germany), the (600 nm)-absorbance (spectrophotometer Evolution 60, Thermo Scientific, Germany) and the concentration of CBZ in the medium. The latter was determined by high pressure liquid chromatography (Hystar Agilent 1200 Series, Germany): Zorbax Eclipse C_{18} column (15 cm × 4.6 mm × 1.8 µm), isocratic elution [60% water : 40% acetonitrile] at 1 mL min^{-1}, injected volume 50 µL, retention time of 7 minutes and UV-absorption detection at 285 nm. The quantification was achieved through a calibration with a series of external standards ranging from 2 to 10 mg L^{-1}.

2.2 Design of Experiments

A central composite design (CCD) of experiments approach of five levels (Fig. 1-b) was adopted (Leustean et al., 2012). It permitted to quickly determine the individual and the combined effects of the two operating conditions (the stirring speed (*SS*) and the gas-to-liquid volume ratio ($R_{G/L}$)) and to determine their critical values leading to extreme (maximum and minimum) performance of the system. Each point of this design corresponded to one combination $SS \times R_{G/L}$ verified by one of the cultures (except the central point (0; 0) corresponding to a four times repeated culture). The *SS* was coded by variable X_1 and the $R_{G/L}$ by variable X_2. The mathematical relationships linking the real variables values to the coded variables were (Eqs. 1-2):

$$SS\ /\ rpm = 100\ X_1 + 200 \quad (1)$$

$$R_{G/L} = (5)^{X_2} \quad (2)$$

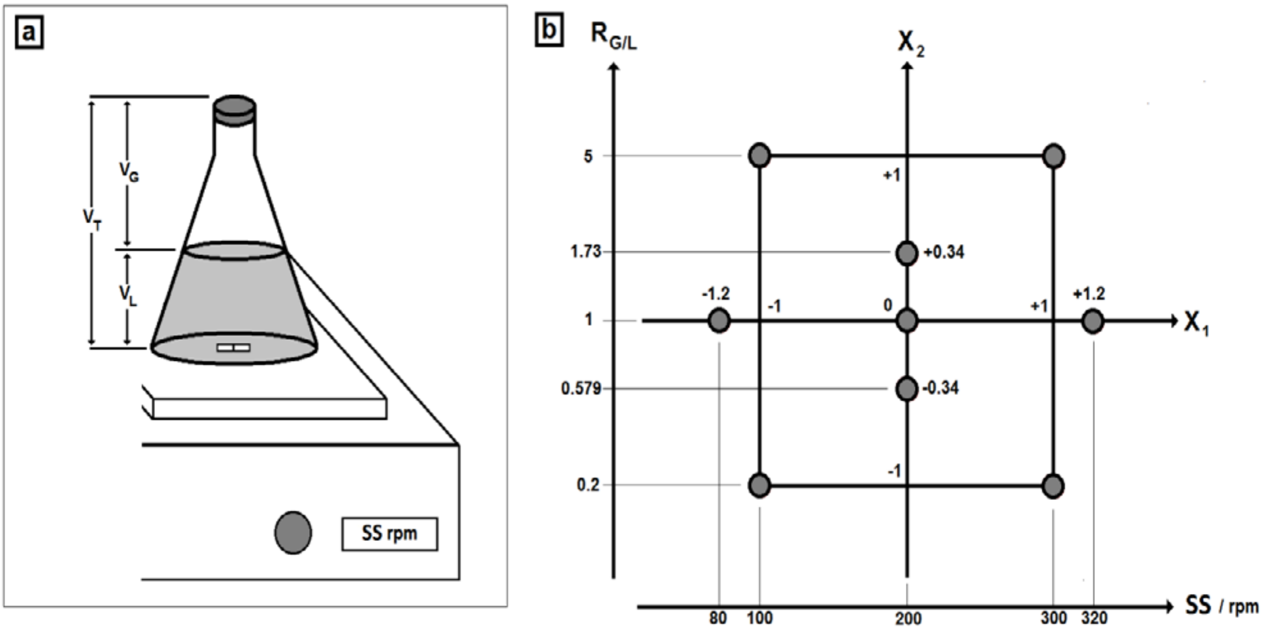

Fig. 1. (a) Schema explaining the operating conditions of a culture. (b) The central composite design of experiments used in this study

3. Results and discussion

3.1. Modeling results

Variation time courses of three parameters (the pH of the medium, the (600 nm)-absorbance and the concentration of CBZ) were modeled (Deriase et al., 2013) for each culture by the three functions $pH(t)$, $A(t)$ and $C(t)$, respectively.

Concerning $pH(t)$, because the observed values presented a weak fluctuation, a linear function of time was chosen to fit it (Eq. 3):

$$pH(t) = a_{pH}\, t + pH_0 \qquad (3)$$

While pH_0 was the initial pH value already prefixed to 7, the slope a_{pH} indicates the average daily change of pH during the 21 days of culture. A positive or negative value of a_{pH} indicates the formation of alkaline or acidic products respectively. The variation over time of the (600 nm)-absorbance was noted as $A(t)$ and modeled by an exponential saturation function (Mason et al., 2006), describing gradual move towards an upper limit (Eq. 4):

$$A(t) = (A_{21} - A_0)\,(1 - e^{-\alpha t}) + A_0 \qquad (4)$$

where A_0 and A_{21} were the measured values of (600 nm)-absorbance at instants $t = 0$ and $t = 21$ days, respectively. A_0 was already prefixed to 0.05 AU when seeding the culture medium. The parameter α is a pseudo-first order kinetic constant, describing the evolution of the medium (600 nm)-absorbance. This absorbance is conventionally used as an indicator of the medium turbidity correlated to biomass concentration. The accuracy of this conventional expectation is discussed through the obtained results.

The decrease in time of the CBZ concentration $C(t)$ was modeled by a bounded negative exponential function of parameter β describing the gradual evolution towards a lower limit (Eq. 5):

$$C(t) = C_{21} + (C_0 - C_{21})\, e^{-\beta t} \qquad (5)$$

The concentrations C_0 and C_{21}, measured respectively at the beginning and at the end of the culture duration, allowed to calculate the CBZ abatement percentage noted $Y\%$ as (Eq. 6):

$$Y\% = (1 - C_{21} / C_0) \times 100\% \qquad (6)$$

For each of the 12 cultures performed, the values of the kinetic parameters a_{pH}, α and β, obtained using the models shown in Eqs. (3), (4) and (5) respectively, were calculated and collected in Table 1. By plotting the parity graph (Fig. 2) representing the modeled values of pH, (600 nm)-absorbance and CBZ concentration versus the corresponding experimental values, a good alignment of the points on the $y = x$ bisector was noticed. Therefore, the considered models adequately described the experimental results with coefficients of determination $R^2 > 0.90$.

The experimental CBZ abatement percentages during the 21 days of culture $Y\%$ (calculated from Eq. 6) are also shown in the penultimate column of Table 1. A response surface was modeled (RSM) by a second degree transfer equation to express $Y\%$ depending on the linear terms X_1 and X_2, the interaction term $X_1 X_2$ and the quadratic terms X_1^2 and X_2^2. The variance analysis presented in Table 2, indicated that the fitted model was statistically meaningful with p-values < 0.05 for all terms, showing the significance of all terms.

The lack of fit was not significant and the equation could be used to navigate the design space. Moreover, according to the $R^2 = 99.5\%$ and Adjusted $R^2 = 99.1\%$, the determination coefficients were high, implying that in the studied domain more than 99% of the response variability was explained by the mathematical expression. Prediction $R^2 = 94.4\%$ was also high indicating a high predictive capacity of the model. The modeled values of $Y\%$ are shown in the last column of Table 1.

Table 1. Results of modeling obtained for the different points of the central composite design (CCD)

Real coordinates		***Coded coordinates***		***pH model***	***(600 nm)-absorbance model***		***CBZ degradation model***		***Abatement Y%***	
SS / rpm	$R_{G/L}$	X_1	X_2	a_{pH} / (10^{-3} day^{-1})	A_{21}	α / (10^{-3} day^{-1})	C_{21} / (mg L^{-1})	β / (10^{-3} day^{-1})	experimental	modeled
100	0.200	– 1.00	– 1.00	75.8	1.82	185	4.54	112	9.3	9.2
100	5.00	– 1.00	1.00	– 66.9	3.75	277	4.86	46.6	2.9	2.8
200	1.00	0.00	0.00	– 20.1	2.60	162	4.82	56.1	3.5	3.5
200	1.00	0.00	0.00	– 23.3	2.50	190	4.81	47.8	3.7	3.5
300	0.200	1.00	– 1.00	72.6	3.20	180	4.54	116	9.2	9.4
300	5.00	1.00	1.00	– 140	4.80	261	4.93	23.0	1.4	1.4
200	1.73	0.00	0.34	– 16.0	2.90	168	4.89	32.5	2.2	2.6
200	0.579	0.00	– 0.34	34.3	3.00	184	4.74	67.8	5.1	5.1
200	1.00	0.00	0.00	– 15.7	2.80	187	4.81	52.3	3.7	3.5
200	1.00	0.00	0.00	– 18.1	2.70	180	4.82	53.9	3.5	3.5
80	1.00	– 1.20	0.00	– 14.9	1.10	135	4.87	32.5	2.5	2.7
320	1.00	1.20	0.00	– 27.7	3.50	200	4.89	30.5	2.1	2.0

Table 2. Analysis of variance and regression results

Total variance	
df [a]	***SS*** [b]
11	73.99

Regression				
df	***SS***	***MS*** [c]	***F*** [d]	***p*** [e]
5	73.63	14.73	243.9	0.000

Determination coefficients		
R^2	***Adjusted R^2***	***Prediction R^2***
0.9951	0.9910	0.9438

Total error		
df	***SS***	***MS***
6	0.3622	0.0604

Lack of fit				
df	***SS***	***MS***	***F***	***p***
3	0.3222	0.1074	8.056	0.060

Pure Error		
df	***SS***	***MS***
3	0.0400	0.0133

Equation						
	Intercept	**Stirring speed**		**Interaction**	**G/L phases ratio**	
		X_1	X_1^2	$X_1 X_2$	X_2	X_2^2
Coefficient	+ 3.50 ± 0.25	− 0.30 ± 0.23	− 0.82 ± 0.33	− 0.35 ± 0.30	− 3.59 ± 0.29	+ 3.01 ± 0.43
p-value	0.000	0.018	0.001	0.029	0.000	0.000

[a] degree of freedom; [b] Sum of squares; [c] Mean of squares; [d] Fisher means of squares ratio; [e] Significance (p-value).

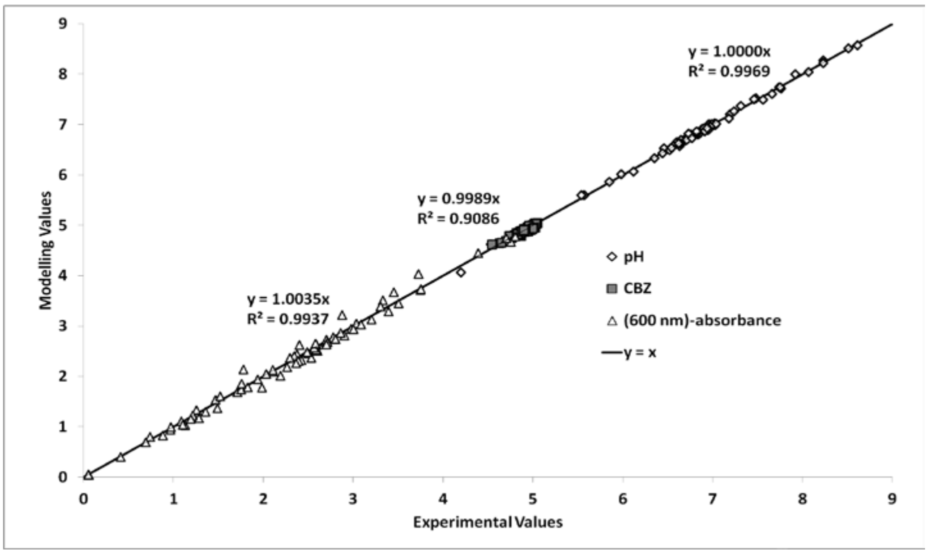

Fig. 2. Parity diagram representing the modeling values versus the experimental values

Pareto chart of the regression model is presented in Fig. 3. As it can be seen in this figure, the gas-to-liquid ratio represents with its linear X_2 and quadratic X_2^2 terms 95.0% of the response variability. On the other hand, the stirring speed represents with its linear X_1 and quadratic X_1^2 terms, together with the interaction term X_1X_2 the remaining 4.5% of the response variability. Consequently, the $R_{G/L}$ effect was considered highly significant, while the *SS* effect was found non-significant.

The modeled equation of the response surface was re-written in terms of the real coordinates *SS* and $R_{G/L}$ in equations (7) and (8):

$$Y\% = 10.1 - \left(\frac{SS-203}{110.43}\right)^2 - \left[\frac{SS}{459.84} + ln\left(\frac{23.4}{R_{G/L}}\right)^{1.16}\right] ln\left(\frac{R_{G/L}}{0.2}\right) \tag{7}$$

$$= 0.62 + ln^2\left(\frac{R_{G/L}}{2.92}\right)^{1.078} + \left[ln\left(\frac{R_{G/L}}{0.2}\right) + \frac{SS-85.3}{26.52}\right]\left(\frac{320-SS}{459.84}\right) \tag{8}$$

Considering Eq. (7), it can be observed that the two negative variable terms vanished if the values SS = 203 rpm and $R_{G/L}$ = 0.2 are plugged in, maximizing *Y%* to 10.1%.

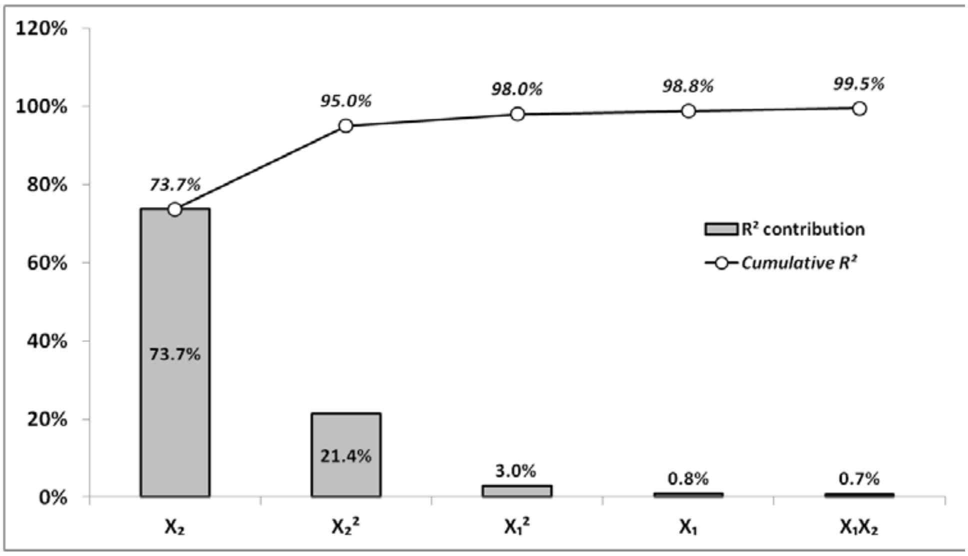

Fig. 3. Pareto chart illustrating the contribution to the determination coefficient R^2 of the stirring speed coded by X_1 and the gas-to-liquid ratio coded by X_2, their squares and interaction

This maximum degradation yield was consistent with those observed in other studies (Gebhardt and Schröder, 2007; Kosjek et al., 2009). Moreover, a higher gas-to-liquid ratio $R_{G/L}$ decreased notably the elimination of CBZ. On the other hand, considering Eq. (8), it can be observed that the two positive variable terms vanished if the values *SS* = 320 rpm and $R_{G/L}$ = 2.92 are plugged in, minimizing *Y%* to 0.62% of degradation. This negligible yield of degradation showed that a high stirring speed had a negative effect on the CBZ elimination especially when the ratio $R_{G/L}$ was high. This could be due to the high content of dissolved oxygen but also to the shear suffered by the biomass cells under the effect of the rotating magnetic bar in a small volume.

It is however noteworthy that in this study, the concentration of seed used for inoculation was very low compared to biomass concentrations usually observed in real activated sludge. This allows to expect better degradation yields if operating at usual biomass concentrations of AS. In addition, the original and positive aspect of this study was to show that the critical operating condition, which led to the best CBZ degradation yield, was to operate in an oxygen deficient atmosphere.

3.2. Results of the principal component analysis

In a second step, Principal Component Analysis (PCA) was applied on seven variables: the design coded variables X_1 and X_2 (stirring speed and gas-to-liquid ratio), the directly read parameters C_{21} and A_{21} (final CBZ concentration and final 600 nm-absorption), and the three modeling kinetic parameters a_{pH}, α and β (pH, 600 nm-absorbance and CBZ evolution) in order to explore and visualize their mutual correlation by reduction of the system dimensionality. The first three principal components *PC1*, *PC2* and *PC3* accounted for 61.56, 23.73 and 12.80% of the total variability respectively and thus the system could be adequately observed in a three dimensional space with losing only 1.91% of the information (Fig. 4).

The seven parameters were then presented in the principal component plans and the observed correlations were visualized in Fig. 4 as follows:

a. The vector representing the stirring speed factor (coded as X_1) is almost perpendicular to the vectors representing C_{21} and β, and hence it has no significant impact on CBZ elimination kinetics.

b. The factor gas-to-liquid ratio (coded as X_2) is positively correlated to C_{21} and negatively correlated to a_{pH} and β (X_2- and C_{21}-vectors are pointing in the direction of positive *PC1*, while a_{pH}- and β-vectors are pointing in the direction of negative *PC1*), which means that a low $R_{G/L}$ led to an increase in pH (alkaline metabolism) and a better elimination kinetics of CBZ, contrarily, a high $R_{G/L}$ led to a decrease of pH (acid metabolism) and a poor elimination kinetics of CBZ.

c. The parameter α describing the increase of the (600 nm)-absorbance is represented by a short vector in both biplots and so it is not significantly correlated to any operating (X_1 and X_2) or kinetic factor (a_{pH} and β). However, certain negative correlation could be observed with the kinetic parameter a_{pH} and so, the (600 nm)-absorbance increased simultaneously with the medium acidity. Because CBZ elimination remained low in acidic conditions, the increased absorbance observed in this case could not be explained by biomass growth as conventionally expected. The formation of a pigment with a highly absorbent acidic form could be hypothesized.

d. The final absorbance A_{21} is presented by a vector almost pointing in the direction of the bisector of the axes *PC1* and *PC2* and shows some positive correlations with its kinetic parameters α and X_1; consequently, high stirring speed induces high (600 nm)-absorbance.

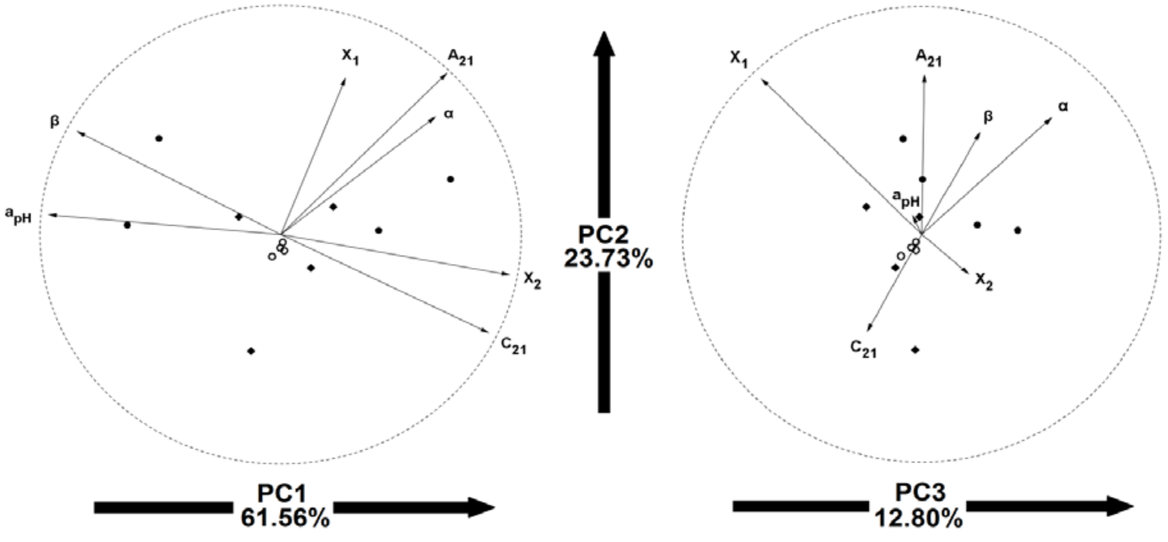

(a) (b)

Fig. 4. Principal component analysis biplots presenting the 7 variables as vectors and the 12 points of the CCD (black circles (●) represent factorial points, white circles (○) represent central points and black rhombuses (♦) represent axial points)(a) in (*PC1*, *PC2*) plan (b) in (*PC3*, *PC2*) plan

3.3. Building a global kinetic model using stepwise-multiple linear regression

Stepwise-multiple linear regression was used to determine the following relationships (Eqs. 9-13):

$$10^3 \times a_{pH} = -13.3 - 13.3X_1 - 88.0X_2 - 17.5X_1X_2; \quad R^2 = 95.4\% \qquad (9)$$

$$10^2 \times A_{21} = 271 + 77.2X_1 + 82.6X_2 + 98.1X_1^2 - 29.2X_2^2; \; R^2 = 93.5\% \qquad (10)$$

$$10^2 \times C_{21} = 482 + 1.37X_1 + 18.0X_2 + 1.75X_1X_2 + 4.08X_1^2 - 14.3X_2^2; \quad R^2 = 99.4\% \qquad (11)$$

$$10^2 \times \alpha A_{21} = 46.4 + 16.2X_1 - 32.1X_2 - 33.8X_2^2; \; R^2 = 92.4\%$$

(11

2)

$$10^3 \times \beta C_{21} = 243 - 15.4X_1 - 177X_2 - 32.8X_1X_2 - 60.6X_1^2 + 160X_2^2; \quad R^2 = 98.0\% \qquad (12)$$

With these equations, the pH, the 600 nm-absorbance and the residual CBZ concentration of every culture at every instant can be calculated by only knowing the stirring speed (80-320 rpm) , the gas-to-liquid ratio (0.2-5) and the time (0-21 days). In fact, the system is completely described by the following set of non-dimensional differential equations (Eq. 13):

$$\frac{1}{a_{pH}} \times \frac{dpH_{(t)}}{dt} = \frac{1}{aA_{21}} \times \frac{dA_{(t)}}{dt} + \frac{A_{(t)}}{A_{21}} = = \frac{1}{\beta C_{21}} \times \frac{aC_{(t)}}{dt} + \frac{C_{(t)}}{C_{21}} = 1 \qquad (13)$$

As a confirmation, the obtained model was used to simulate the evolution of the culture pH, the (600 nm)-absorbance (noted as *A*) and the CBZ concentration (noted as *C*) for two sets of conditions. The results are displayed in Fig. 5.

3.4. Proposing a simplified mechanistic model

To explain the negative effect of abundant oxygen on CBZ elimination accompanied with acidification of the medium, the following thermodynamically possible oxidation reactions were written (Eqs. 14-16):

$$2\ CBZ + O_2 \rightarrow 2\ EP\text{-}CBZ; \ \Delta E^{0'} = 0.97\ V \qquad (14)$$

$$NH_4^+ + 2\ O_2 \rightarrow NO_3^- + H_2O + 2\ H^+; \ \Delta E^{0'} = (0.35 + 0.015\ pH)\ V \qquad (15)$$

$$NO_3^- + 4\ CBZ + 3H_2O \rightarrow NH_4^+ + 4\ EP\text{-}CBZ + 2\ HO^-; \ \Delta E^{0'} = (0.62 - 0.015\ pH)\ V \qquad (16)$$

Despite the high potential of reaction (14), it is not kinetically possible because of the absence of an adequate catalyst/enzyme allowing the transformation of carbamazepine (CBZ) into epoxy-carbamazepine (EP-CBZ) directly by adding molecular oxygen to the double bond.

Moreover, no significant elimination of CBZ was observed in the presence of abundant oxygen and the acidification of the medium in this case could be explained by Eq. (15) where two hydrogen ions are formed. On the other hand, when no abundant oxygen is available, the slow Eq. (16) would occur and explain the alkalization of the medium in this case thanks to the formation of two hydroxide ions.

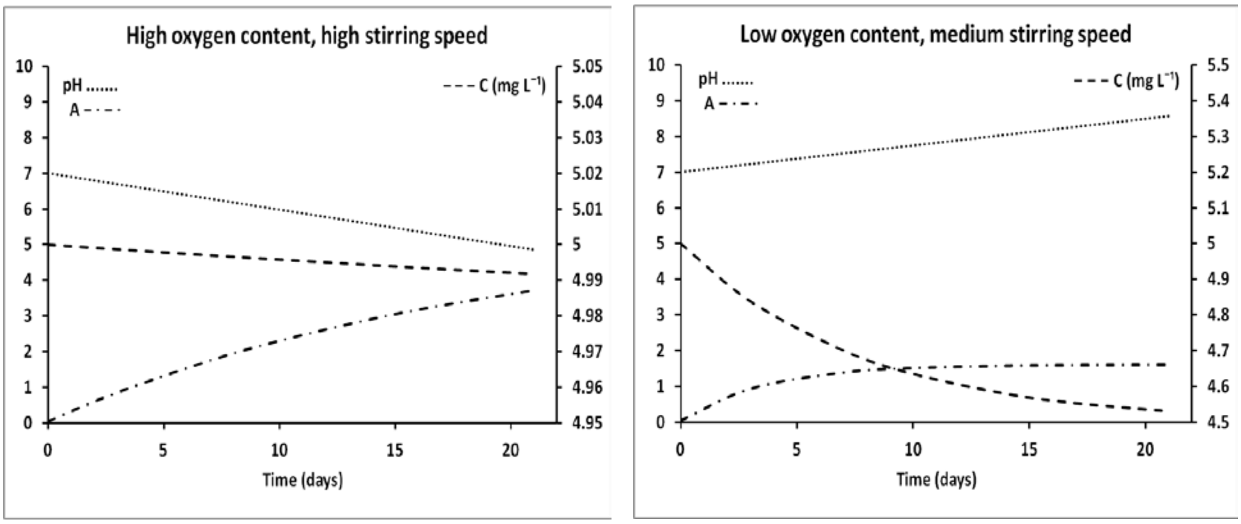

(a) (b)

Fig. 5. Simulation of the evolution of the pH, the (600 nm)-absorbance (noted as *A*), the CBZ concentration (noted as *C*) for two sets of conditions. (a) $R_{G/L}$ = 2.92 and 320 rpm leading to the minimal elimination yield, and (b) $R_{G/L}$ = 0.2 and 203 rpm leading to the maximal elimination yield

In order to explain the increased (600 nm)-absorbance in acidic medium, where CBZ consumption remained low leading to a poor biomass growth, the following mechanism can be supposed:

a. The energy produced by CBZ degradation allow the growth of new biomass BIO with a yield ρ (Eq. 17):

$$[BIO]_{(t)} = \rho\left(C_0 - C_{(t)}\right) + A_0 \tag{17}$$

b. The biomass release a pigment PIG which has an acidity constant pK_a describing its repartition into two forms PIG $_{acid}$ and PIG $_{basic}$ depending on the pH (Eq. 18):

$$pH_{(t)} = pK_a + log\frac{[PIG_{basic}]_{(t)}}{[PIG_{acid}]_{(t)}} \Rightarrow$$
$$[PIG]_{(t)} = [PIG_{acid}]_{(t)}\left(1 + 10^{pH-pKa}\right) \tag{18}$$

c. The (600 nm)-absorbance is the resultant of the biomass concentration and the acid form of the pigment PIG $_{acid}$ absorbance; *u* is a constant accounting for different extinction coefficients (Eq.19):

$$A_{(t)} = [BIO]_{(t)} + u[PIG_{acid}]_{(t)} \Rightarrow$$
$$[PIG]_{(t)} = \frac{\left(A_{(t)} - A_0\right) - \rho\left(C_0 - C_{(t)}\right)}{u} \times (1 + 10^{pH-pKa}) \tag{19}$$

Several combinations of values were tested for the three constants ρ, pK_a and *u*, and the following combination was chosen as the most logical: $\rho \approx 0$, namely no significant biomass growth but only usage of the energy for basal maintenance; $pK_a = 10$, so the acidic form of the pigment (which is the form absorbing at 600 nm) is always the predominant form; and $u = 100$, so the amount of the formed pigment is consistently in the same magnitude as the amount of present biomass.

The proposed model succeeded to explain the controversial increase in (600 nm)-absorbance when no carbon substrate utilization was observed, by assuming that the acidic form of the pigment produced by the biomass in stress situation, was able to absorb light in the same wavelengths range as the biomass. However, the model also showed stable biomass concentration even when some carbamazepine was consumed; biomass was not able to use all the available CBZ to grow maybe because the accumulation of degradation products inhibited the microbial metabolism.

4. Conclusions

The resistance of carbamazepine to treatment by activated sludge was confirmed. However, this study has allowed identifying the major limiting factor that result in the poor elimination of CBZ in WWTP: intensive aeration. Anoxic oxidation of CBZ by nitrate was more efficient than the direct reaction with oxygen.

Another limiting factor was the slow kinetics due to the absence of the adequate enzymes; a possible solution would be to find microbial strains able to produce such enzymes and add them to the activated sludge to achieve a bioaugmentation process (Semrany et al., 2012).

Abbreviations

CBZ: carbamazepine / $K_{o/w}$: distribution coefficient octanol-water / **WWTP**: wastewater treatment plant / **UV**: ultraviolet / **AS**: activated sludge / ***SS***: stirring speed / $R_{G/L}$: gas-to-liquid ratio / **CCD**: central composite design / **AU**: absorbance unit / **RSM**: response surface methodology /

PCA: principal component analysis **/ PIG**: pigment / **BIO**: biomass.

Acknowledgements

This paper is published as part of the PhD thesis of the first author (S. Semrany) which is supported by both the Lebanese university and the Lebanese social association Azm and Saadeh.

References

Andreozzi R., Raffaele M., Nicklas P., (2003), Pharmaceuticals in STP effluents and their solar photodegradation in aquatic environment, *Chemosphere*, **50**, 1319-1330.

Chen M.X., Fang H., Qi R., He S.X., Wei Y.S., (2016), 17B-estradiol degrading bacteria in sequencing batch reactors for swine wastewater treatment, *Environmental Engineering and Management Journal*, **15**, 2273-2278.

Clara M., Strenn B., Kreuzinger N., (2004), Carbamazepine as a possible anthropogenic marker in the aquatic environment: investigations on the behaviour of Carbamazepine in wastewater treatment and during groundwater infiltration, *Water Research*, **38**, 947-954.

Crini G., Badot P.-M., (2008), *Treatment and purification of polluted industrial water: Membrane processes, bioadsorption and chemical oxidation*, (in French),University Franche-Comté Publisger, France

Deriase S.F., Younis S.A., El-Gendy N.S., (2013), Kinetic evaluation and modeling for batch degradation of 2-hydroxybiphenyl and 2, 2′-dihydroxybiphenyl by *Corynebacterium variabilis* Sh42, *Desalination and Water Treatment*, **51**, 4719-4728.

Ferrari B., Mons R., Vollat B., Fraysse B., Paxēaus N., Giudice R.L., Pollio A., Garric J., (2004), Environmental risk assessment of six human pharmaceuticals: Are the current environmental risk assessment procedures sufficient for the protection of the aquatic environment?, *Environmental Toxicology and Chemistry*, **23**, 1344-1354.

Gebhardt W., Schröder H.F., (2007), Liquid chromatography-(tandem) mass spectrometry for the follow-up of the elimination of persistent pharmaceuticals during wastewater treatment applying biological wastewater treatment and advanced oxidation, *Journal of Chromatography A*, **1160**, 34-43.

Jones O.A.H., Voulvoulis N., Lester J.N., (2002), Aquatic environmental assessment of the top 25 English prescription pharmaceuticals, *Water Research*, **36**, 5013-5022.

Kosjek T., Andersen H.R., Kompare B., Ledin A., Heath E., (2009), Fate of Carbamazepine during Water Treatment, *Environmental Science & Technology*, **43**, 6256-6261.

Leustean I., Coman G., Bahrim G., (2012), Statistical optimisation of ethanol production from a cellulosic mixture based on paper residues, *Environmental Engineering and Management Journal*, **11**,1037-1044.

Mason I.G., McLachlan R.I., Gérard D.T., (2006), A double exponential model for biochemical oxygen demand, *Bioresource Technology*, **97**, 273–282.

Metcalfe C.D., Miao X.-S., Koenig B.G., Struger J., (2003), Distribution of acidic and neutral drugs in surface waters near sewage treatment plants in the lower Great Lakes, Canada, *Environmental Toxicology and Chemistry*, **22**, 2881-2889.

Ozkan-Yucel U.G., Gokcay C.F., (2017), Modeling of dye reduction by sludge digestion: combined effect of biochemical and chemical reduction, *Environmental Engineering and Management Journal*, **16**, 1543-1550.

Öllers S., Singer H.P., Fässler P., Müller S.R., (2001), Simultaneous quantification of neutral and acidic pharmaceuticals and pesticides at the low-ng/l level in surface and waste water, *Journal of Chromatography A*, **911**, 225-234.

Rehman M.S.U., Saif A., Rashid A., Mahmood T., (2013), Chemometric classification of advanced oxidation processes for the degradation of pharmaceuticals and personal care products, *Environmental Engineering and Management Journal*, **12**, 475-481.

Rizzo L., (2011), Bioassays as a tool for evaluating advanced oxidation processes in water and wastewater treatment, *Water Research*, **45**, 4311-4340.

Scheytt T., Mersmann P., Lindstädt R., Heberer T., (2005), Determination of sorption coefficients of pharmaceutically active substances carbamazepine, diclofenac, and ibuprofen, in sandy sediments, *Chemosphere*, **60**, 245-253.

Semrany S., Favier L., Djelal H., Taha S., Amrane A., (2012), Bioaugmentation: Possible solution in the treatment of Bio-Refractory Organic Compounds (Bio-ROCs), *Biochemical Engineering Journal*, **69**, 75-86.

Ternes T.A., (1998), Occurrence of drugs in German sewage treatment plants and rivers, *Water Research*, **32**, 3245-3260.

Ternes T.A., (2001), *Pharmaceuticals and Care Products in the Environment*, American Chemical Society, New York. 39-54.

Ternes T.A., Meisenheimer M., McDowell D., Sacher F., Brauch H.-J., Haist-Gulde B., Preuss G., Wilme U., Zulei-Seibert N., (2002), Removal of pharmaceuticals during drinking water treatment, *Environmental Science & Technology*, **36**, 3855-3863.

Yehya T., Favier L., Kadmi Y., Audonnet F., Fayad N., Gavrilescu M., Vial C., (2015), Removal of carbamazepine by electrocoagulation: investigation of some key operational parameters, *Environmental Engineering and Management Journal*, **14**, 639-645.

Yu S.Y., Zhang G.M., Li J.Z., Wan T., (2016), Can disintegration based on COD (DDCOD) represent the biodegradability of disintegrated sludge?, *Environmental Engineering and Management Journal*, **15**, 1737-1742.